International Journal of Nanomedicine

Dovepress
open access to scientific and medical research

Open Access Full Text Article

ORIGINAL RESEARCH

Riclin-Capped Silver Nanoparticles as an Antibacterial and Anti-Inflammatory Wound Dressing

Changchang Kong, Shijunyin Chen, Wenhao Ge, Yang Zhao, Xiaodong Xu, Shiming Wang, Jianfa Zhang

Center for Molecular Metabolism, Nanjing University of Science & Technology, Nanjing, Jiangsu, 210094, People's Republic of China

Correspondence: Jianfa Zhang, Center for Molecular Metabolism, Nanjing University of Science & Technology, 200 Xiaolingwei, Nanjing, 210094, People's Republic of China, Tel/Fax +86 25 84318533, Email jfzhang@njust.edu.cn

Purpose: In order to overcome the inflammatory response to bacterial infection during wound healing, we have fabricated an antibacterial and anti-inflammatory wound dressing based on polysaccharide riclin and silver nanoparticles (AgNPs).

Methods: The riclin-AgNPs nanocomposite was developed by borohydride method and was characterized by UV-Vis, TEM, XRD, Zeta potential, DLS. In vitro, we assessed the cumulative release, antibacterial activities and cytotoxicity. In vivo, we examined the wound healing in mice wound infection experiment and inflammatory mediators using histological observations and gene expression analysis.

Results: The riclin/AgNPs nanocomposite hydrogel exhibited nanosized orbicular particles with high purity and stability. In vitro, the riclin/AgNPs showed sustained release of AgNPs, effective suppression in pathogen growth and negligible toxicity toward mammalian fibroblasts and macrophage cells. In vivo, the riclin/AgNPs treatment leads to faster and smoother growth of fresh skin with suppressed expression of inflammatory mediators.

Conclusion: The reported Riclin-AgNPs nanocomposite hydrogel showed both antibacterial and anti-inflammatory functions, which induce significantly accelerated wound healing, indicating great potential as a novel attractive wound dressing material.

Keywords: nanocomposite hydrogels, wound healing, riclin, silver nanoparticles

Introduction

Wound healing is a very complex and dynamic process involving sequential molecular, physiological, biochemical, and cellular processes that replace damaged structures with new cells and tissues.[1] In both acute and chronic wounds, the healing process begins with circulating inflammatory mediators penetrating the wound site, growth factors and extracellular matrix secretion, which initiate epithelial regeneration, connective tissue contraction, and angiogenesis to rebuild the damaged epidermis and dermis.[2] Infections and inflammatory responses would impact the healing process of severe injuries. Therefore, choosing a suitable wound dressing material is crucial to provide temporary protection during wound healing and treatment to replace damaged skin.

The most common wound dressings are gauze and cotton balls, but these traditional ones have inherent shortages,[3] such as easy adhesion to the wound and weak barrier function. The ideal wound dressing should inhibit microbial invasion, mitigate inflammatory response, accelerate wound closure, inhibit scar formation and be economical.[1] A large number of experimental studies have found moderately moist environments accelerate the healing process because they are more suitable for cell proliferation than dry environments according to the widely accepted theory of wet wound healing. Hydrogel is a polymer material with a network structure and hydrophilic groups inside, which can absorb a large amount of water and be firmly combined with water.[4] Thus, hydrogel medical dressing is regarded as a new type of wound dressings.[5–7] Compared with traditional dressings, it can improve the micro-environment, relieve pain, and promote wound healing.[8]

Riclin is a succinoglycan-like polysaccharide from an *Agrobacterium* isolate and is composed of galactose and glucose residues at a ratio of 1:7, along with two modifications succinate and pyruvate.[9] The molecular weight of riclin is approximately 2.5×10^6 Da. Due to the hydroxyl groups, especially diols on the side chain, the riclin can be cross-linked via a borate complex of

Received: 17 March 2022
Accepted: 7 June 2022
Published: 13 June 2022

two diols.[10] Riclin exhibits excellent anti-inflammatory properties in vitro and in vivo,[11] which may work as an anti-inflammatory hydrogel used in wound healing. In addition, hydrogel materials can maintain the physical and mechanical qualities of an ideal wound dressing material while carrying various compounds. Therefore, antibacterial factors are usually added to hydrogel to meet the requirements of ideal medical wound dressings.[4] Recently, nanomaterials are constantly being used as novel antibacterial factors against infectious pathogens and remodeled in the field of medicine.[12]

It is well known that AgNPs show a broad antibacterial spectrum against both gram-positive and gram-negative bacteria amongst various antibacterial agents, and bacterial resistance to AgNPs has not been observed in clinically relevant pathogens.[13] Although the specific mechanisms through which AgNPs exert their antimicrobial effects are still under investigation, nanoparticles are reported to kill the microbes by disrupting the integrity of the cell membrane and cellular respiration.[14] In addition to these physical interplays, the release of silver ions (Ag^{+}) is considered an essential mechanism for the bactericidal effect of AgNPs.[15] It also has the ability to produce poisonous reactive oxygen species (ROS) inside the bacterial cell,[16] and oxidative damage caused by the generation of ROS is considered a critical antimicrobial mechanism.[17] Besides its antibiotic and multilevel antimicrobial activities (multidrug resistance),[18] AgNPs are also well known for their low systemic toxicity.[19] Therefore, many studies have been conducted on the development of silver nanocomposite hydrogels for biomedical applications during the last few years,[12,20,21] which have been widely used to fabricate medicated wound dressings.[22]

Considering that polysaccharides can form environment-friendly and bio-compatibility hydrogels,[23] we hypothesized that the anti-inflammatory polysaccharide riclin could be a good backbone for antibacterial AgNPs. In this work, we aimed to fabricate and characterize AgNPs-loaded riclin hydrogel with $NaBH_4$, which work as reducing agent during the synthesis of AgNPs and form the borate as cross-linkers during the fabrication of riclin hydrogel.[24] Then, we investigated their promoting effects in anti-bacteria and accelerating wound closure, expected to provide a new wound healer.

Materials and Methods

Materials

The silver nitrate (>99% $AgNO_3$) and sodium borohydride (99% $NaBH_4$) were purchased from Aldrich Chemical Company. The strain Agrobacterium sp. ZCC3656 was cultivation in modified M9 salts medium, and Riclin was purified by heat-alkaline method for usage in animal experiments. The detail is same as described in previously shown.[25] The total carbohydrate content of the purified riclin was greater than 95% and the proteins were undetected. The murine macrophage cell line (RAW 264.7) and mouse skin fibroblast cell line (NIH3T3) were obtained from the Centre of Cellular Resource, Chinese Academic of Sciences (Shanghai, China).

Synthesis of AgNPs and Riclin/AgNPs Biocomposite

AgNPs were synthesized using the chemical reduction of $AgNO_3$ with $NaBH_4$ as a reducing and stabilizing agent. First, 0.8 g riclin was solubilized in 30 mL of deionized water. Then, sodium borohydride (up to 2 mM final concentration) was added, and the mixture was slightly stirred followed by frozen in an ice bath. At last, 10 mL volume of 1.0 mM silver nitrate dropwise (about 1 drop/sec) was added. The reaction mixture was stirred firmly on a magnetic stirring plate and the mixture turned golden yellow. The entire adding process took about five minutes; then, we stopped stirring and removed the stirring rod.[26] The formation of AgNPs was observed by visual inspection of the color change of the solution.

Characterization of AgNPs and Riclin/AgNPs Biocomposite

Ultraviolet-Visible (UV-Vis) Spectroscopy

UV-Vis spectrophotometer (PowerWave XS, BioTek, USA) was used as a monitor for in-situ synthesis of AgNPs, in which wavelength was measured from 300 nm to 600 nm.

Transmission Electron Microscopy (TEM)

The size and morphological examinations of synthesized AgNPs were achieved by transmission electron microscopy (TEM) (JEM-2100F, JEOL, Japan) with an acceleration voltage of 200 kV. For the TEM measurements, the AgNPs powder was suspended in ethanol and then a drop of colloidal solution containing synthesized AgNPs was dropped on a

carbon-coated copper grid and was loaded onto a specimen holder. Digital Micrograph software was calibrated for AgNPs size measurements using a digital TEM camera.

Dynamic Light Scattering (DLS) and Zeta Potential

The size distributions of the AgNPs were assessed by Dynamic Light Scattering (DLS), and stability was assessed by Zeta potential using a Nano-ZS Zeta sizer apparatus (Malvern Instruments, United Kingdom). Smolukovsky equation was adopted in order to calculate the Zeta potential from the electrophoretic mobility analysis. Data obtained were analyzed using Zetasizer software.

X-Ray Diffraction (XRD)

XRD patterns of the AgNPs and nanocomposite were examined by X-ray diffractometer (D8 Advance, Bruker, Germany) operated at a voltage of 40 kV and a current of 40 mA. The crystalline structure of AgNPs was characterized in 2θ range of 10°-80°. The peaks obtained were assigned and compared with the database published by the Joint Committee on Powder Diffraction Standards (JCPDS).

Moisture Retention Measurement

In order to measure the moisture retention capacity of the hydrogel, hydrogel was weighted (m_0), placed in an incubator allowing good ventilation at 37°C and then weighted (m_w) at specific time intervals. The moisture retention time was recorded until m_w stop changing. The moisture retention rate was calculated using the following equation:

Moisture retention (%) = $(m_w - m_0)/m_0 \times 100$.

Ag^+ Release Measurement and Degradation Test of Riclin/AgNPs Hydrogel

Silver quantification by ICP-MS. AgNP fraction mixed with concentrated sub-boiled HNO_3 plus 30% (w/v) H_2O_2 was subjected to microwave-assisted decomposition. Then, the decomposed samples were diluted with 0.2% (v/v) HNO_3, and the silver was determined by ICP-MS.

For the in vitro degradation test, a 0.5-mL riclin/AgNPs hydrogel was prepared and placed on a plate with 20 mL PBS (pH 7.4) at room temperature. At the scheduled time, the whole solution and hydrogel were placed in 50 mL weighted centrifuge tube and centrifuged at 10,000 rpm for 10 min, and then the supernatant was placed back on the plate and the centrifuge tube was weighted to record the remaining gel weight (W_t).[27] The degradation ratio of hydrogels was then defined by the following equation:

Degradation ratio (%) = $(W_t\text{-}W_0)/W_0*100\%$

Where W_0 is the gel weight measured at 0 h.

Antibacterial Activity

The antibacterial activities of riclin and the riclin/AgNPs biocomposite were determined by inhibition-zone and optical density (OD600) measurements. The bacterial strains of *S. aureus* and *E. coli* were selected as representatives of Gram-positive and Gram-negative species recognized as skin commensals, as well as nosocomial pathogens.

The antibacterial activities of riclin and riclin/AgNPs hydrogels were evaluated using OD values measured in real-time by a Bacterial Growth Curves Meter (Karroten Scientific, Nanjing, China). Bacteria were incubated in these two samples with various concentrations (10 μg/mL, 20 μg/mL) at 37°C for 24 h. The absorbance has an inversely proportional relationship with antibacterial efficiency. The obtained OD600 values were subtracted from the samples themselves to exclude any possible interference.

The antibacterial activities of silver-loaded hydrogel agents were evaluated via the inhibition-zone method. Briefly, the agar plates were inoculated with the freshly grown bacterial suspensions (1×10^8 CFU/mL) by the aseptic technique. Then, an 8 mm round agar disc was replaced with 100 uL riclin or riclin/AgNPs hydrogels in each plate, and the plates were incubated at 37°C for 24 h. Finally, the diameters of the bacterial inhibition zones on the medium surfaces were measured.

In vitro Study of Riclin/AgNPs Cytotoxicity Toward Mouse Fibroblasts Cells and Macrophage Cells

The cell viability of riclin and riclin/AgNPs hydrogels was tested via the MTT assay on mouse skin fibroblast (NIH3T3) cells and macrophage (Raw 264.7) cells.[11,24] The conventional MTT (3-[4,5-dimethylthiazol-2-yl]-2,5-diphenyltetrazolium bromide) method was performed for the cell proliferation assay. RAW 264.7 cells were seeded into 96-well plates and incubated at 37°C in 5% CO_2 for 12 h, and NIH3T3 cells were seeded into 96-well plates at a density of 1×10^4 cell per mL and incubated at 37°C in 5% CO_2 for 24 h. The cells were treated by a culture medium (Dulbecco's modified Eagle's medium (DMEM)) with different concentrations of AgNPs or riclin hydrogel loaded with different concentrations of AgNPs for 24 h, with each concentration assayed using four replicate wells. Subsequently, 10 μL of MTT (Sigma-Aldrich, St. Louis, MO) solution (5 mg mL^{-1}) was added to each well and incubated at 37°C for 4 h. Then, the culture supernatant was carefully removed and dimethyl sulfoxide (150 μL) was added to each well. The absorbance was measured at 570 nm using a microplate reader (Thermo Fisher Scientific).

Cell viability (%) = $OD_{treated}/OD_{control} \times 100$

where $OD_{treated}$ is the absorbance of cells treated by sample, and $OD_{control}$ is the absorbance of cells treated by culture medium without AgNPs.

Animal Models

We chose the full-thickness skin defect model to assess wound healing. All animal studies were performed in accordance with the Guide for Care and Use of Laboratory Animals. Specifically, eighteen male C57 BL/6 mice (22 ± 2 g) aged 6 to 8 weeks were housed in a temperature- and humidity-controlled room under a 12 h light-12 h dark cycle. All the mice could drink and eat freely in an SPF environment. All animal experiments and care were approved by the Institutional Animal Care and Use Committee at the Nanjing University of Science and Technology (ACUC-NUST-20160016). All mice were intraperitoneally injected with 0.1 mL/100 g of 4% chloral hydrate for general anesthesia and then randomly divided into three groups, each with six mice. Shave the hair on the back of each mouse with an electric shaver. Then, the limbs were fixed on the animal operating table, and the skin was disinfected with 75% alcohol. An infected wound was created by cutting off the round skin of 1 cm in diameter on the mouse's back and injecting 50 μL of *S. aureus* bacterial suspension (turbidity: 0.5) onto the defected areas. After that, different interventions were performed on the wounds. The first wound served as a control and was untreated, while the other wounds were covered with riclin or riclin/AgNPs. All wounds were covered with 3M Tegaderm™ Film. The dressing materials were changed every two days. Twelve days later, one mouse from each group was sacrificed and half of their fresh granulation tissues were excised completely. Half of the granulation tissues were promptly immersed in 10% neutral formaldehyde for H&E and Masson staining.

On days 0, 4, 8, and 12, digital cameras were used to photograph the healing process of each group. The formula for calculating the wound healing rate is as follows:

Wound healing rate = $(S_0\text{-}S_i)/ S_0 \times 100\%$

Table 1 Primer Sequences Used for Real-Time RT-PCR

Gene	Forward/Reverse	Primer (5' to 3')
GAPDH	Forward	CATCCACTGGTGCTGCC AAGGCTGT
	Reverse	ACAACCTGGTCCTCAGTGTAGCCCA
IL-1β	Forward	CATCCAGCTTCAAATCTCGCAG
	Reverse	CACACACCAGCAGGTTATCATC
TNF-α	Forward	ACGGCATGGATCTCAAAGAC
	Reverse	CGGACTCCGCAAAGTCTAAG
IL-6	Forward	CATGTTCTCTGGGAAATCGTGG
	Reverse	GTACTCCAGGTAGCTATGGTAC
Col1A1	Forward	ACGTCCTGGTGAAGTTGGTC
	Reverse	CAGGGAAGCCTCTTTCTCCT

where S_0 represents the original number of pixels at the wound site, and S_i represents the number of pixels at the wound site at the time of measurement.

Gene Expression Analysis of Inflammatory Mediators in Wounds

The gene expression of the inflammatory mediators (interleukin 6 (IL-6), interleukin 1beta (IL-1β), tumor necrosis factor alpha (TNF-α), collagen protein 1 (CollA1)) was estimated in the wound tissues treated with hydrogels of riclin and riclin/AgNPs and the untreated control for 8 days. The inflammatory state of regenerative tissues was investigated using Quantitative Real time-PCR. Total RNA was extracted from the skin with the Karrol reagent from Karroten Scientific (Nanjing, Jiangsu, China) following the manufacturer's instructions. RNA was converted to cDNA using reverse transcript kits from Invitrogen (Carlsbad, CA, USA). Quantitative real-time PCR was performed with the cDNA using an Applied Biosystems 7300 real-time PCR system. Primer sequences used for quantitative RT-PCR are shown in Table 1. The relative gene expression in comparison with GAPDH expression was calculated by the ΔΔCT (comparative cycle threshold) method.

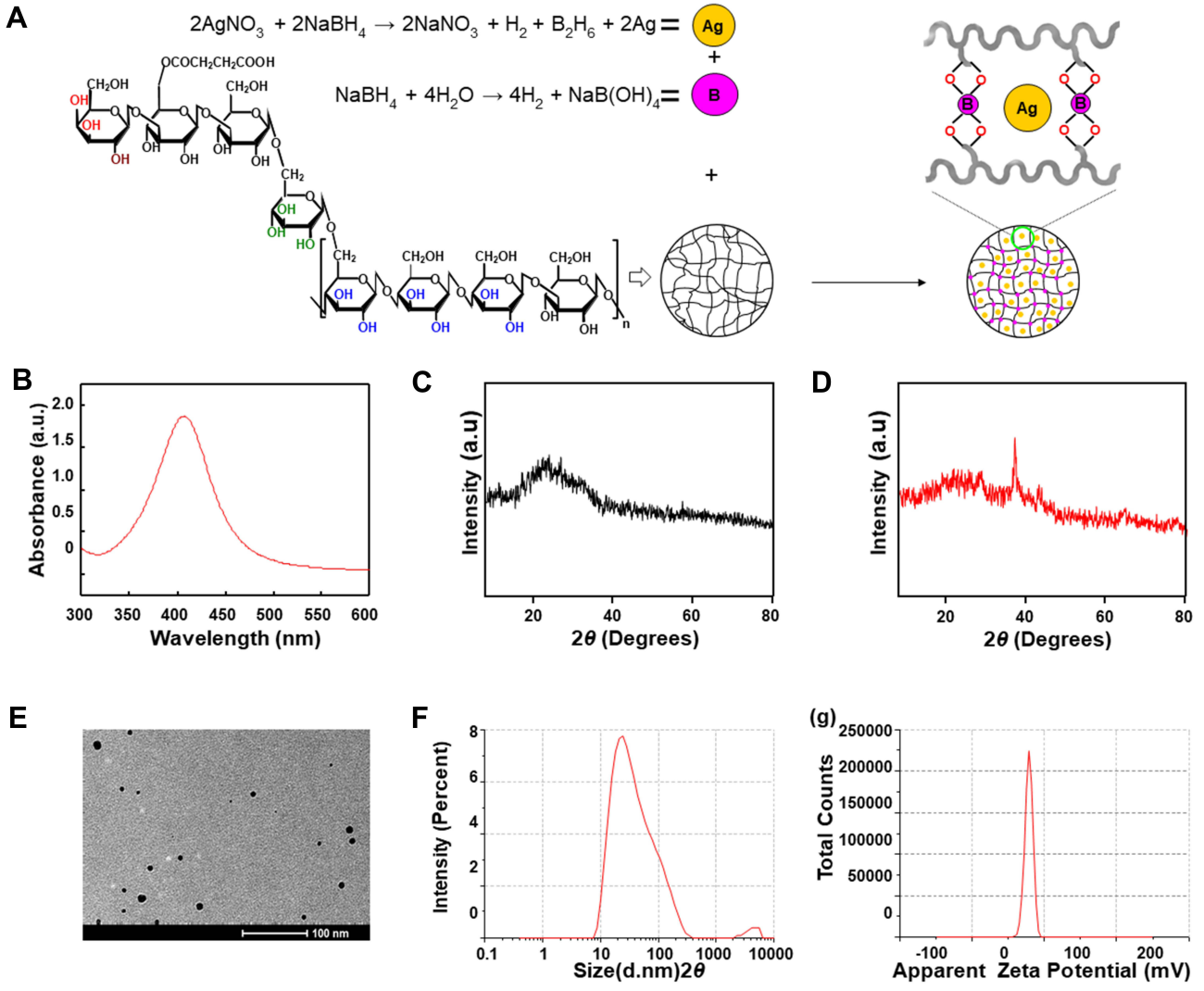

Figure 1 (**A**) Graphic illustration of preparation mechanism of riclin, and riclin/AgNPs hydrogels; (**B**) UV–vis absorption spectra of aqueous dispersions of AgNPs; (**C**) XRD pattern of riclin hydrogels; (**D**) XRD pattern of riclin/AgNPs hydrogels; (**E**) TEM images of AgNPs; (**F**) Particle size distribution of AgNPs; (**G**) Zeta potential of the synthesized AgNPs.

Statistical Analysis

All data are expressed as means ± standard deviations. All results were analyzed for statistical significance by Student's *t*-test or 1-way analysis of variance. Results with P values of less than 0.05 were considered statistically significant. Asterisk *, ** and *** denotes the statistical significance of $P < 0.05$, $P < 0.01$ and $P < 0.001$, respectively.

Results and Discussion

Fabrication of Nanocomposite Hydrogels and Characterization of Silver Nanoparticles

The structure of riclin and the preparation procedures of riclin/AgNPs nanocomposite hydrogel are shown in Figure 1A. A supramolecular riclin/AgNPs nanocomposite hydrogel was obtained by the borohydride method.[28] Furthermore, $NaBH_4$ exists in the form of $B(OH)_4^-$ in an aqueous solution and it can react with up to four hydroxyl groups, thus allowing cross-linking reactions to occur even at lower concentrations.[29] The formation of AgNPs was observed visually through the changes in the solution color and a sharp peak range of 380–430 nm from the UV-visible spectrum (Figure 1B). The XRD pattern of riclin and riclin/AgNPs is shown in Figure 1C and D, which demonstrates the purity and physical structure of the formed AgNPs. The higher intensity of the plane (111) indicates that the structure of the synthesized AgNPs is predominantly orientated in this plane.[30] As seen in Figure 1E, the obtained AgNPs were orbicular in shape having a homogenous distribution

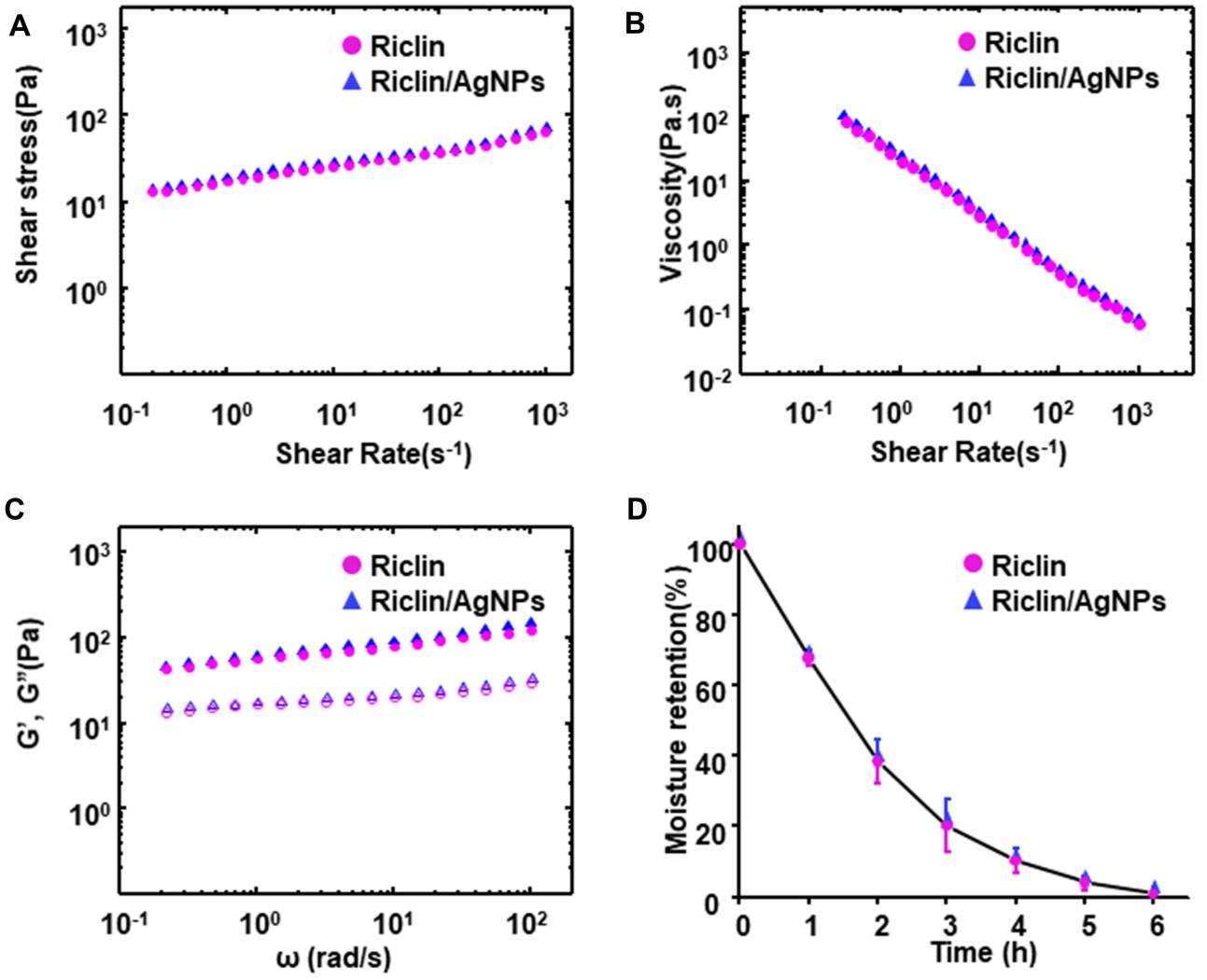

Figure 2 Rheological and moisture retention properties of pristine riclin and riclin/AgNPs hydrogel. (**A**) Shear stress of the samples per weight as a function of the shear rate; (**B**) viscosity vs shear rate; (**C**) storage modulus (*G'*, solid symbols) and loss modulus (*G''*, hollow symbols) as a function of the strain amplitude; (**D**) moisture retention curve of riclin and riclin/AgNPs hydrogel.

with the primary average size from 10 nm to 20 nm under a TEM microscope. The main average size of the AgNPs was 25.92 nm using DLS in Figure 1F. The size measured by DLS can be larger because the size obtained from DLS depends not only on the metallic core of nanoparticles but also on substances absorbed on NP surfaces.[31] The average zeta potential value was found to be −21.4mv in Figure 1G. It is known that the surface charge prevents the nanoparticle from aggregation by providing electrostatic repulsion to the similarly charged nanoparticles in their neighborhood.[32] Thus, the high negative potential value of the nanoparticle afforded long-term stability, good colloidal nature, and high dispersity to the AgNPs.[33,34] These results proved the successful synthesis of the Ag nanoparticles, and the in-situ synthesized AgNPs were composed of crystalline silver with high purity and stability.

Rheological and Moisty Retention Properties of Riclin/AgNPs Nanocomposite Hydrogel

The high mole weight (2.5×10^6 Da) of riclin results in a high shear viscosity and moisture retention capacity of the hydrogel shown in Figure 2. All samples exhibited shear thinning with pseudoplastic flow behavior in Figure 2A and B. Figure 2C shows the storage modulus (*G*') and loss modulus (*G*") graphs as a function of the strain amplitude of each riclin-based sample at a fixed angular frequency (ω) of 10 rad/s. All the hydrogels exhibited relatively small strain amplitudes and exhibited a slightly dominant (solid-like) *G*'. Therefore, riclin/AgNPs hydrogel could maintain a gel-like structure and resist small shear stresses, such as gravity or brushing to secondary dressings. The agreeable adhesive strength makes the hydrogel suitable as a wound sealant.[6] These properties are desirable as wound dressings should be able to maintain adequate viscosity at the wound site to avoid excessive flow.[35] Good tissue adhesion ensures that the dressing can always be closely attached to the wound bed and reduces the threat of external damage caused by the falling off of the dressing.[7] The riclin shows good moisture retention characteristics in

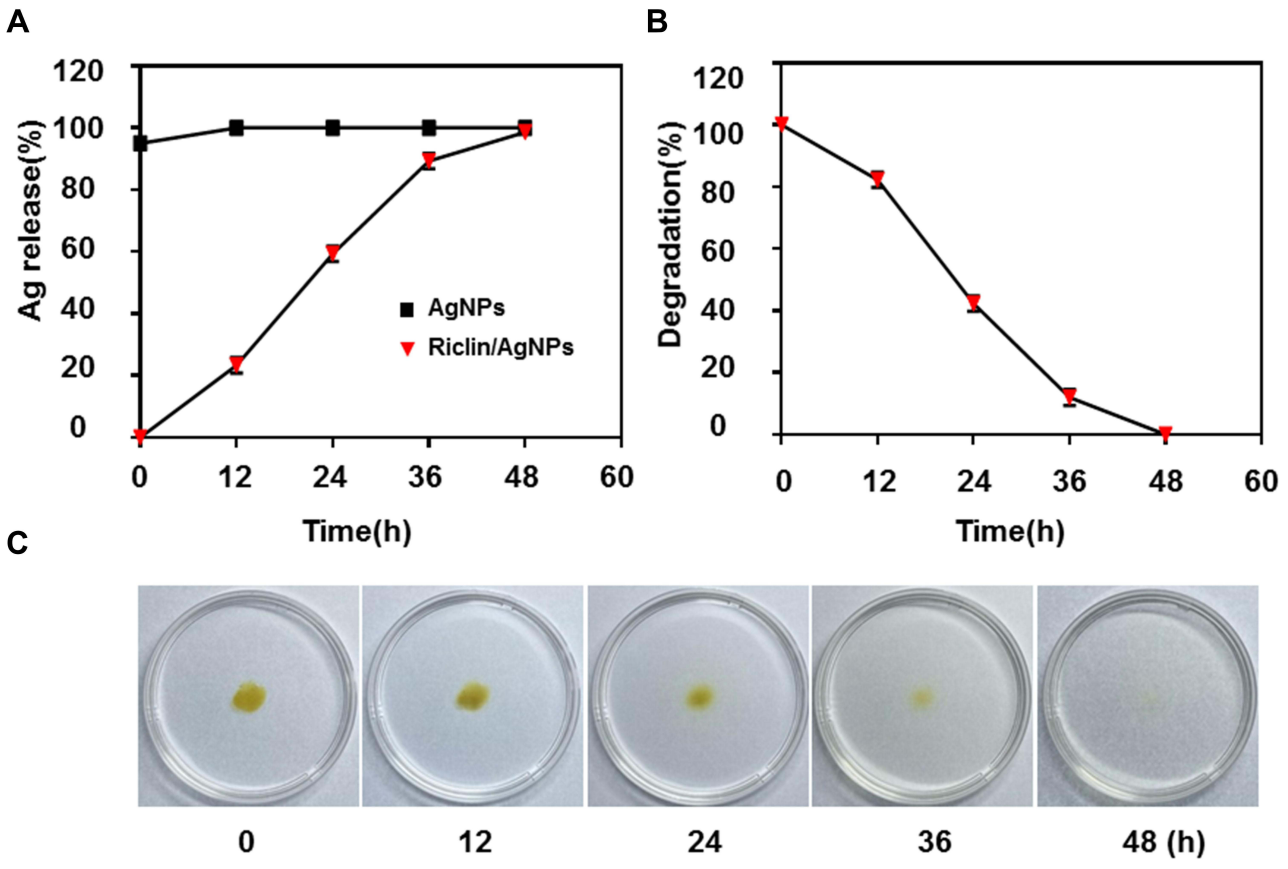

Figure 3 (**A**) In vitro release of AgNPs are compared between control (AgNPs) and treatment (riclin/AgNPs). Loading of AgNPs into hydrogel was resulted in a prolonged release pattern of the nanoparticles over 48 hours of exposure; (**B**) in vitro degradation of riclin/AgNPs hydrogel. (**C**) The pictures of riclin/AgNPs hydrogel at different degradation time.

Figure 2D, due to the hydrogen bond formed by succinyl residues and hydroxyl groups with water.[36] According to the moist wound healing theory, moist wound treatment could promote wound healing, remove the dressing painlessly without destroying freshly formed tissue and reduce scar formation.[37]

Ag^+ Release of Silver Nanoparticles and Degradation of Riclin/AgNPs Hydrogel

The release behavior of AgNPs upon loading into riclin hydrogel was investigated as demonstrated in Figure 3A, the release pattern of the AgNPs loaded into riclin hydrogel was slow and constant over the first 24 h. An almost complete release of the AgNPs was shown after 48 h of exposure. The in vitro degradation test showed similar trend in Figure 3B and C. We proposed that loading the AgNPs into riclin hydrogel extended their contact time with the wounded area and prolonged their release, which was supposed to maximize the wound healing effect and minimize side effects. The sustained release of AgNPs from these nanocomposite hydrogels was probably due to the firm capture of the metal form of silver (AgNP) in the cross-linked riclin matrix. Sustained release of AgNPs was one of the most desirable properties for the hydrogels as wound dressing materials, and it was reported that the utilization of AgNPs loaded hydrogel had decreased the cytotoxicity and increased duration of the therapeutic effect.[38]

In vitro Antibacterial Activity

Uncontrolled bacterial proliferation on the wound surface might delay the healing process from inflammation to the remodeling stage.[39] Thus, removing the infectious agent from the wound bed is necessary. The growth curves of *E. coli* and *S. aureus* treated with AgNPs are shown in Figure 4A and B. Under the absence of AgNPs, *E. coli* reached the

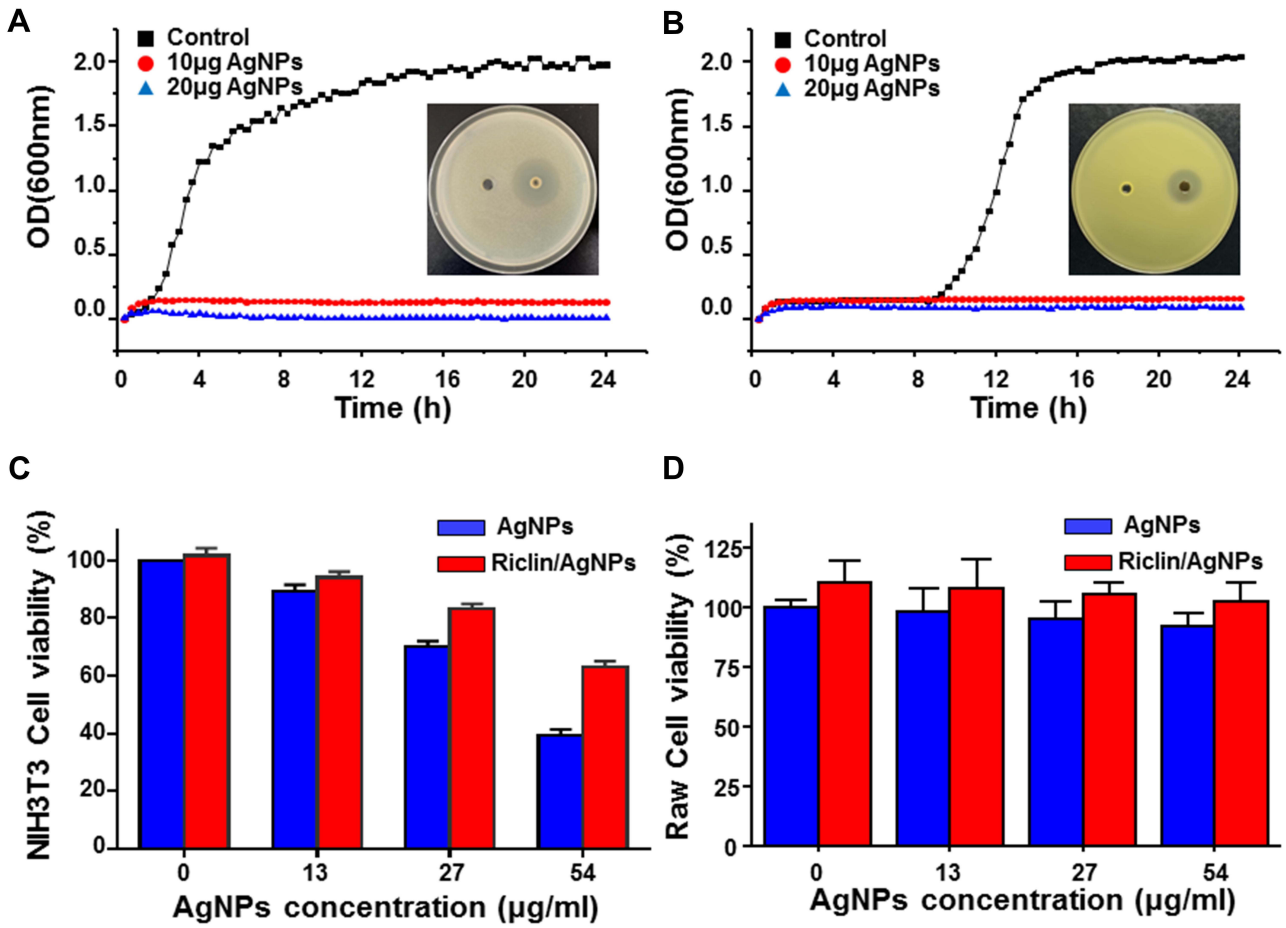

Figure 4 Antibacterial activity of pristine riclin and riclin/AgNPs hydrogels against *E. coli* (**A**) and *S. aureus* (**B**); all data are presented by the mean ± standard deviation (SD, n = 3) ($p < 0.05$); Viability of NIH3T3 mouse fibroblasts (**C**) and Raw 264.7 (**D**) after 24-h exposure to different concentrations of AgNPs and riclin/AgNPs composed hydrogel.

exponential phase rapidly. When exposed to 10 and 20 μg/mL of AgNPs, the OD value of *E. coli* gradually decreased from 4 hours to 24 hours, indicating that the bactericidal concentration of AgNPs to *E. coli* was 10 μg/mL. The growth of *S. aureus* was basically the same as that of *E. coli* when exposed to 20 μg/mL AgNPs. When exposed to a dose of 10 μg/mL, the growth is almost stagnant, indicating that the inhibitory concentration of AgNPs to *S. aureus* was 10 μg/mL. No inhibition zone was observed for riclin hydrogel, suggesting that riclin had no antimicrobial activity. On the contrary, riclin/AgNPs exhibited remarkable antibacterial activity against both *E. coli* and *S. aureus*.

The viability levels of mouse skin fibroblasts NIH3T3 and macrophage cells after exposure to various concentrations of test samples are shown in Figure 4C and D. Riclin/AgNPs composed hydrogels obtained no significant cytotoxicity at concentrations of 0 to 27 μg/mL, whereas AgNPs showed similar results only at a dose of 0~13 μg/mL. Riclin/AgNPs composed hydrogels exhibited weak cytotoxicity (>60% cell viability) toward NIH3T3 mouse fibroblasts at concentrations of 54 μg/mL. However, riclin/AgNPs show no impact on raw cells at this dose. Therefore, conjugation of riclin to $B(OH)_4^-$ indirectly influenced the cytotoxicity of the composed hydrogels. In general, riclin/AgNPs composed hydrogels were less toxic than the AgNPs. As reported by ISO 10993–5 (ISO, 2009), percentages of cell viability above 80% are considered non-cytotoxic. Thus, the negligible toxicity of riclin/AgNPs toward NIH3T3 mammalian fibroblasts and macrophage cells confirmed its potential use for the treatment of bacteria-infected wounds, showing that our Ag-releasing riclin hydrogels were suitable for thematic application as wound-healing agents for the treatment of infected wounds.

In vivo Wound Healing Under Infection of *S. aureus*

In the mice models, we found that riclin/AgNPs composed hydrogel were able to promote the infected wound repair in Figure 5A and B. The dressing of riclin/AgNPs was chosen as a sample to estimate in vivo wound healing potential and compared with pure

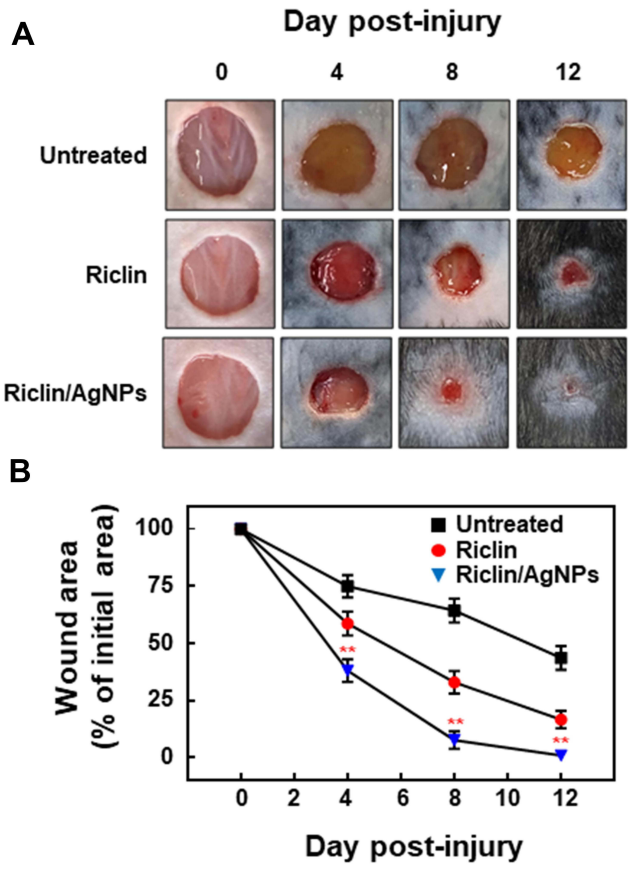

Figure 5 Effect of test samples on the healing of *S. aureus*-infected wounds in C57BL/6 mice. (**A**) Representative photographs of the healing of *S. aureus*-infected wounds treated with riclin or riclin/AgNPs. (**B**) Percentage of the area reduction of mouse skin lesions relative to the initial wound. Data are the mean ± standard deviation (n = 6); *P < 0.05, compared with the untreated group.

riclin and bare in Figure 5. The dressing of riclin/AgNPs showed an excellent healing effect as early as the fourth day after operation compared with other groups. Moreover, the growing fresh skin after riclin/AgNPs treatment appeared smoother and left less scab than treated with riclin and blank control. The area of wound closure at different healing times was also quantified, and the result was shown in Figure 5B. Four days after the operation, the wound treated with riclin/AgNPs appears to have meaningful closure to 62%, whereas the wounds treated with riclin and blank control show 25% and 41% wound closure, respectively. After 12 days of healing, the wound closure of riclin/AgNPs treated was 100%, which was about 17% higher than that of the riclin and 180% higher than untreated. The complete wound closure was observed as early as day 12 for riclin/AgNPs, while it was 14 days for riclin. For blank control, the time required for a complete wound closure is more than 16 days.

Histological Observations and Gene Expression Analysis of Inflammatory Mediators

We next examined the histological characterization of the wound tissue after eight days of treatment. The H&E stained images revealed that the riclin/AgNPs appeared to have complete re-epithelialization and intact epidermis, while the untreated wounds were not fully closed (Figure 6A, upper). Several granulation tissues are observed on the bare and

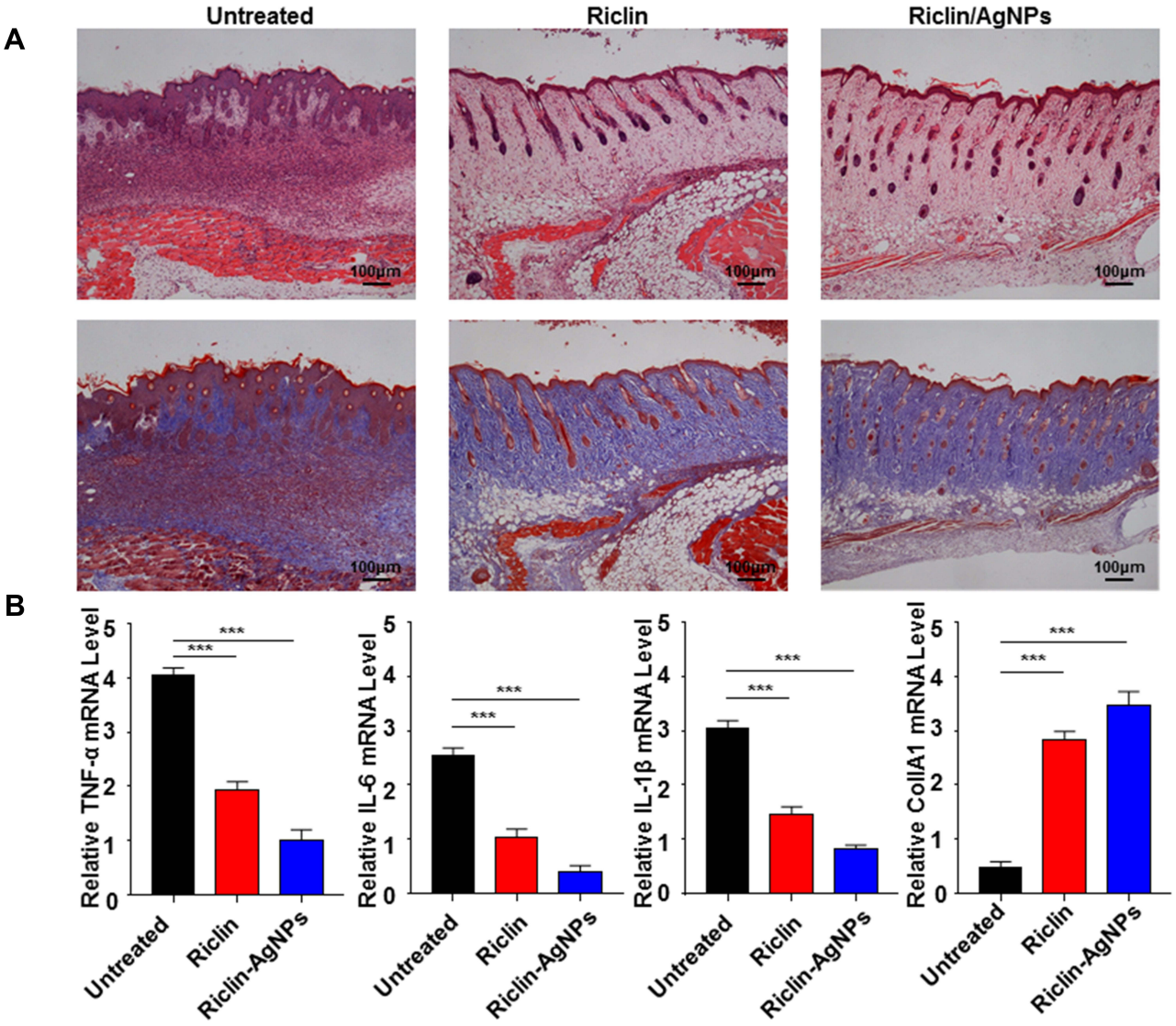

Figure 6 (**A**) Histological (H&E and MT staining) analysis of *S. aureus*-infected wounds in C57BL/6 mice. Scale bar = 100 μm; H&E, hematoxylin and eosin; MT, Masson's trichrome. Red arrows indicate blood vessels; blue arrows indicate early epithelialization, pink arrows indicate fibroblasts, and Orange arrows indicate mononuclear inflammatory cells. The blue color in the MT-stained tissue indicates collagen, arranged parallel to the skin surface. (**B**) Gene expression analysis of IL-6, IL-1β, TNF-α inflammatory mediators in wounds treated with hydrogels of riclin and riclin/AgNPs after 8 days of treatment. Data are presented as mean ± SD, n = 3. One-way ANOVA was used to evaluate the statistical differences, ***Represents $p < 0.001$.

riclin treated wounds (marked with black arrows). Nevertheless, for the group treated with riclin/AgNPs, the granulation tissue was organized into fibrous connective tissue. Moreover, the accumulation of keratinocytes in wounds treated with riclin/AgNPs was much denser than that treated with riclin and bare. The above results indicated the enhanced wound tissue repair capability of the riclin/AgNPs dressing. To exhibit the degree of collagen deposition, the Masson stained images are shown in Figure 6A (down), in which the collagen was stained into blue. After eight days of healing, the wounds treated with riclin/AgNPs were much denser than those treated with riclin and bare. In summary, riclin/AgNPs show excellent wound repairing ability, which could promote re-epithelization, profit the organization of granulation tissue and accelerate the wound healing process accordingly.

Figure 6B indicates that the pro-inflammatory factors, TNF-α, IL-6, IL-1β, were maintained at low levels when treated by the riclin/AgNPs composed hydrogels but CollA1 at high levels. Following dressing application, the inflammation was maintained at a low level of balance, reducing the risk of wound chronicity.[17] In the wound healing process, macrophages play a vital role in cell proliferation, collagen deposition, vascularization and granulation by the secretion of various cytokines and chemokines.[40] The expression of the IL-1α gene was significantly ($P < 0.05$) decreased in the riclin/AgNPs group, while IL-6 expression was down-regulated in the riclin group, but the level was not significant. Both IL-1α and IL-6 mRNA expression was lowered in the riclin and riclin/AgNPs group. Hence, after riclin or riclin/AgNPs treatment, increased expression of CollA1 had suppressed the inflammatory cytokines (IL-1α and IL-6) and promoted the healing process effectively.

Conclusion

A novel nano riclin/AgNPs composite hydrogel was successfully prepared by the in-situ reduction method. In vitro and in vivo antibacterial studies demonstrate tremendous antibacterial activity against pathogenic bacteria. In vivo evaluation in mice confirmed that the riclin/AgNPs dressings appeared to have faster wound healing, more complete re-epithelialization and denser collagen deposition characteristics. These results demonstrated that riclin/AgNPs have great promise in future clinical application as a new and safe wound dressing.

Acknowledgments

This work was supported by the National Natural Science Foundation of China (31871178) and the Fundamental Research Funds for the Central Universities (30920031102).

Disclosure

The authors report no conflicts of interest in this work.

References

1. Shankar S, Jaiswal L, Aparna RSL, Prasad RGV, Kumar GP, Manohara CM. Wound healing potential of green synthesized silver nanoparticles prepared from Lansium domesticum fruit peel extract. *Mater Express*. 2015;5(2):159–164. doi:10.1166/mex.2015.1225
2. Lin S-P, Kung H-N, Tsai Y-S, Tseng T-N, Hsu K-D, Cheng K-C. Novel dextran modified bacterial cellulose hydrogel accelerating cutaneous wound healing. *Cellulose*. 2017;24(11):4927–4937. doi:10.1007/s10570-017-1448-x
3. Song R, Zheng J, Liu Y, et al. A natural cordycepin/chitosan complex hydrogel with outstanding self-healable and wound healing properties. *Int J Biol Macromol*. 2019;134:91–99. doi:10.1016/j.ijbiomac.2019.04.195
4. Chen K, Wang F, Liu S, Wu X, Xu L, Zhang D. In situ reduction of silver nanoparticles by sodium alginate to obtain silver-loaded composite wound dressing with enhanced mechanical and antimicrobial property. *Int J Biol Macromol*. 2020;148:501–509. doi:10.1016/j.ijbiomac.2020.01.156
5. Dhivya S, Padma V, Elango S. Wound dressings – a review. *BioMedicine*. 2015;5. doi:10.7603/s40681-015-0022-9
6. Liang Y, Li Z, Huang Y, Yu R, Guo B. Dual-dynamic-bond cross-linked antibacterial adhesive hydrogel sealants with on-demand removability for post-wound-closure and infected wound healing. *ACS Nano*. 2021;15(4):7078–7093. doi:10.1021/acsnano.1c00204
7. Liang Y, Li M, Yang Y, Qiao L, Xu H, Guo B. pH/glucose dual responsive metformin release hydrogel dressings with adhesion and self-healing via dual-dynamic bonding for athletic diabetic foot wound healing. *ACS Nano*. 2022;16(2):3194–3207. doi:10.1021/acsnano.1c11040
8. Liang M, Liwen Z, Yun Z, Yanbo D, Jianping C. The imbalance between Foxp3(+)Tregs and Th1/Th17/Th22 cells in patients with newly diagnosed autoimmune hepatitis. *J Immunol Res*. 2018;2018:3753081. doi:10.1155/2018/3753081
9. Yang Y, Sun X, Zhao Y, et al. Anti-tumor activity and immunogenicity of a succinoglycan riclin. *Carbohydr Polym*. 2021;255:117370. doi:10.1016/j.carbpol.2020.117370
10. Bishop M, Shahid N, Yang J, Barron AR. Determination of the mode and efficacy of the cross-linking of guar by borate using MAS 11B NMR of borate cross-linked guar in combination with solution 11B NMR of model systems. *Dalton Trans*. 2004;17:2621–2634. doi:10.1039/B406952H

11. Cheng R, Wang L, Li J, Fu R, Wang S, Zhang J. In vitro and in vivo anti-inflammatory activity of a succinoglycan Riclin from Agrobacterium sp. ZCC3656. *J Appl Microbiol*. 2019;127(6):1716–1726. doi:10.1111/jam.14447
12. Wahid F, Khan T, Shehzad A, Ui-Islam M, Kim YY. Interaction of nanomaterials with cells and their medical applications. *J Nanosci Nanotechnol*. 2014;14(1):744–754. doi:10.1166/jnn.2014.9016
13. Maharjan B, Joshi MK, Tiwari AP, Park CH, Kim CS. In-situ synthesis of AgNPs in the natural/synthetic hybrid nanofibrous scaffolds: fabrication, characterization and antimicrobial activities. *J Mech Behav Biomed Mater*. 2017;65:66–76. doi:10.1016/j.jmbbm.2016.07.034
14. Kvítek L, Panáček A, Soukupová J, et al. Effect of surfactants and polymers on stability and antibacterial activity of Silver Nanoparticles (NPs). *J Phys Chem C*. 2008;112(15):5825–5834. doi:10.1021/jp711616v
15. Chernousova S, Epple M. Silver as antibacterial agent: ion, nanoparticle, and metal. *Angew Chem Int Ed Engl*. 2013;52(6):1636–1653. doi:10.1002/anie.201205923
16. Wan Y, Zhang D, Wang Y, Qi P, Wu J, Hou B. Vancomycin-functionalised Ag@TiO2 phototoxicity for bacteria. *J Hazard Mater*. 2011;186(1):306–312. doi:10.1016/j.jhazmat.2010.10.110
17. Shahverdi AR, Fakhimi A, Shahverdi HR, Minaian S. Synthesis and effect of silver nanoparticles on the antibacterial activity of different antibiotics against Staphylococcus aureus and Escherichia coli. *Nanomedicine*. 2007;3(2):168–171. doi:10.1016/j.nano.2007.02.001
18. Azizi S, Namvar F, Mahdavi M, Ahmad MB, Mohamad R. Biosynthesis of silver nanoparticles using brown marine macroalga, sargassum muticum aqueous extract. *Materials*. 2013;6(12):5942–5950. doi:10.3390/ma6125942
19. Fong J, Wood F. Nanocrystalline silver dressings in wound management: a review. *Int J Nanomedicine*. 2006;1(4):441–449. doi:10.2147/nano.2006.1.4.441
20. Juby KA, Dwivedi C, Kumar M, Kota S, Misra HS, Bajaj PN. Silver nanoparticle-loaded PVA/gum acacia hydrogel: synthesis, characterization and antibacterial study. *Carbohydr Polym*. 2012;89(3):906–913. doi:10.1016/j.carbpol.2012.04.033
21. Reddy PR, Varaprasad K, Sadiku R, et al. Development of gelatin based inorganic nanocomposite hydrogels for inactivation of bacteria. *J Inorg Organomet Polym Mater*. 2013;23(5):1054–1060. doi:10.1007/s10904-013-9886-x
22. Ambrogi V, Donnadio A, Pietrella D, et al. Chitosan films containing mesoporous SBA-15 supported silver nanoparticles for wound dressing. *J Mater Chem B*. 2014;2(36):6054–6063. doi:10.1039/C4TB00927D
23. Zhu T, Mao J, Cheng Y, et al. Recent progress of polysaccharide-based hydrogel interfaces for wound healing and tissue engineering. *Adv Mater Interfaces*. 2019;6(17). doi:10.1002/admi.201900761
24. Palem RR, Madhusudana Rao K, Kang TJ. Self-healable and dual-functional guar gum-grafted-polyacrylamidoglycolic acid-based hydrogels with nano-silver for wound dressings. *Carbohydr Polym*. 2019;223:115074. doi:10.1016/j.carbpol.2019.115074
25. Yang Y, Sun Q, Xu X, et al. Oral administration of succinoglycan riclin improves diet-induced hypercholesterolemia in mice. *J Agric Food Chem*. 2019;67(48):13307–13317. doi:10.1021/acs.jafc.9b06034
26. Babaei Z, Rezaei B, Pisheh MK, Afshar-Taromi F. In situ synthesis of gold/silver nanoparticles and polyaniline as buffer layer in polymer solar cells. *Mater Chem Phys*. 2020;248:122879. doi:10.1016/j.matchemphys.2020.122879
27. Han X, Meng X, Wu Z, Wu Z, Qi X. Dynamic imine bond cross-linked self-healing thermosensitive hydrogels for sustained anticancer therapy via intratumoral injection. *Mater Sci Eng C Mater Biol Appl*. 2018;93:1064–1072. doi:10.1016/j.msec.2018.08.064
28. Li N, Liu C, Chen W. Facile access to guar gum based supramolecular hydrogels with rapid self-healing ability and multistimuli responsive gel-sol transitions. *J Agric Food Chem*. 2019;67(2):746–752. doi:10.1021/acs.jafc.8b05130
29. Bocchinfuso G, Mazzuca C, Sandolo C, et al. Guar gum and scleroglucan interactions with borax: experimental and theoretical studies of an unexpected similarity. *J Phys Chem B*. 2010;114(41):13059–13068. doi:10.1021/jp105838t
30. Kanmani P, Lim ST. Synthesis and structural characterization of silver nanoparticles using bacterial exopolysaccharide and its antimicrobial activity against food and multidrug resistant pathogens. *Process Biochem*. 2013;48(7):1099–1106. doi:10.1016/j.procbio.2013.05.011
31. Chand K, Cao D, Eldin Fouad D, et al. Green synthesis, characterization and photocatalytic application of silver nanoparticles synthesized by various plant extracts. *Arab J Chem*. 2020;13(11):8248–8261. doi:10.1016/j.arabjc.2020.01.009
32. Biswal AK, Misra PK. Biosynthesis and characterization of silver nanoparticles for prospective application in food packaging and biomedical fields. *Mater Chem Phys*. 2020;250:123014.
33. Das P, Ghosal K, Jana NK, Mukherjee A, Basak P. Green synthesis and characterization of silver nanoparticles using belladonna mother tincture and its efficacy as a potential antibacterial and anti-inflammatory agent. *Mater Chem Phys*. 2019;228:310–317. doi:10.1016/j.matchemphys.2019.02.064
34. Jyoti K, Baunthiyal M, Singh A. Characterization of silver nanoparticles synthesized using Urtica dioica Linn. leaves and their synergistic effects with antibiotics. *J Radiat Res Appl Sci*. 2019;9(3):217–227. doi:10.1016/j.jrras.2015.10.002
35. Matthews KH, Stevens HN, Auffret AD, Humphrey MJ, Eccleston GM. Gamma-irradiation of lyophilised wound healing wafers. *Int J Pharm*. 2006;313(1–2):78–86. doi:10.1016/j.ijpharm.2006.01.023
36. Xu X, Chen A, Ge X, Li S, Zhang T, Xu H. Chain conformation and physicochemical properties of polysaccharide (glucuronoxylomannan) from Fruit Bodies of Tremella fuciformis. *Carbohydr Polym*. 2020;245:116354. doi:10.1016/j.carbpol.2020.116354
37. Hinman CD, Maibach H. Effect of Air Exposure and Occlusion on Experimental Human Skin Wounds. *Nature*. 1963;200(4904):377–378. doi:10.1038/200377a0
38. Akkari ACS, Papini JZB, Garcia GK, et al. Poloxamer 407/188 binary thermosensitive hydrogels as delivery systems for infiltrative local anesthesia: physico-chemical characterization and pharmacological evaluation. *Mater Sci Eng C Mater Biol Appl*. 2016;68:299–307. doi:10.1016/j.msec.2016.05.088
39. Hasan N, Lee J, Kwak D, et al. Diethylenetriamine/NONOate-doped alginate hydrogel with sustained nitric oxide release and minimal toxicity to accelerate healing of MRSA-infected wounds. *Carbohydr Polym*. 2021;270:118387. doi:10.1016/j.carbpol.2021.118387
40. You C, Li Q, Wang X, et al. Silver nanoparticle loaded collagen/chitosan scaffolds promote wound healing via regulating fibroblast migration and macrophage activation. *Sci Rep*. 2017;7(1):10489. doi:10.1038/s41598-017-10481-0